A R C H I V E S O F M E T A L L U R G Y A N D M A T E R I A L S
Volume 60 2015 Issue 2
DOI: 10.1515/amm-2015-0137

D.-S. KIM*, V. DHAND*, K.-Y. RHEE*,♯, S.-J. PARK**

SURFACE TREATMENT AND MODIFICATION OF GRAPHENE USING ORGANOSILANE AND ITS THERMAL STABILITY

OBRÓBKA POWIERZCHNIOWA I MODYFIKACJA GRAFENU PRZY UŻYCIU ORGANOSILANU I JEGO STABILNOŚĆ TERMICZNA

In this study, graphene was functionalized via acid oxidation in the presence of a mixture of concentrated sulfuric acid and nitric acid. The oxidized graphene was silanized using the coupling agent, 3-aminopropyltriethoxsilane, resulting in functionalized graphene. The oxidized graphene and functionalized graphene were characterized by X-Ray diffraction, Fourier transform infrared spectroscopy, High-resolution micro Raman spectroscopy, thermogravimetric analysis, and atomic force microscopy to confirm the presence of functional moieties on the graphene surface. Thermal studies also demonstrate that the functionalized material is thermally stable up to higher temperatures.

Keywords: Graphite, Thermal Properties, Raman Spectroscopy, Surface Treatment, 3-APTES

1. Introduction

Graphene is a monolayer of carbon atoms arranged in a two-dimensional honeycomb lattice, and exhibits excellent mechanical and electrical properties. The superior mobility, thermal and electrical conductivity and room-temperature ballistic transport makes it an attractive material for electric, optoelectronic and photonic devices. In particular, graphene satisfies all requirements for a good field emission source due to its atomic thickness, high aspect ratio, excellent electrical conductivity and good mechanical properties [1-11]. Furthermore, graphene has been found to outperform carbon nanotubes (CNTs) as a reinforcing filler [12] and also has good biocompatibility with the foreign additives [13]. For these reasons, graphene has been studied in diverse fields of physics, chemistry and engineering since the last few years. However, two problems must be overcome when dealing with polymers reinforced with graphene. The first problem is the dispersion of graphene within the polymer matrix. The second is the poor interfacial adhesion between graphene and the matrix. Kathi and Rhee (2008) proposed silanization of functionalized (oxidized) carbon nanotubes as a preferred method of enhancing the interfacial adhesion between the nanotubes and the matrix [14]. Furthermore, the structures of silanized CNTs remained largely intact, indicating that no real damage occurred to the CNTs during the silanization process. Ma et al (2006) reported a similar result after examining the silanization of CNTs using 3-glycid-oxy-propyl-trimethoxysilane [15]. As mentioned above, silanization is an effective method for improving the interfacial adhesion between the nanomaterial and the matrix. Therefore, it is expected that graphene silanization will improve the interfacial adhesion between graphene and the host matrix.

In the present study, 3-aminopropyltriethoxysilane (3-APTES) was used as the silane coupling agent to treat graphene. 3-APTES is an important aminosilane that has many applications in nylon, phenolic, epoxy, and melamine resin-based composites. Graphene was functionalized by oxidation with a mixture of concentrated nitric acid and sulfuric acid. The functionalized graphene was chemically modified by covalently bonding the 3-APTES molecule with the oxidized graphene, in hopes of improving their compatibility with other polymers for diverse applications in graphene-based polymer matrix composite industries.

2. Experimental

2.1. Reagents

Raw graphene powder (Grade AO-3) used in this study was purchased from Graphene Supermarket synthesized using a catalytic chemical vapor deposition (CVD) process which had an average thickness of 12nm, and purity above 99%. 3-aminopropyltriethoxysilane (3-APTES), with 99% purity (Aldrich), was used as the silane functionalization agent. The following reagents were used without further purification: sulfuric acid (95%, Dae Jung Chemicals, Korea), nitric acid (70%, MS, Osaka, Japan), acetone (99.5%, Dae Jung Chemicals, Korea), and ethanol (99.5+%, Sigma-Aldrich).

* DEPARTMENT OF MECHANICAL ENGINEERING, KYUNG HEE UNIVERSITY, 1732 DEONGYEONG-DAERO, YONGIN-SI, GYEONGGI 446-701, KOREA
** DEPARTMENT OF CHEMISTRY, INHA UNIVERSITY, 253 NAM-GU, INCHEON, 402-751, KOREA
♯ Corresponding author: rheeky@khu.ac.kr

2.2. Oxidation of graphene

Three grams of graphene was dispersed in 300mL of a concentrated H2SO4:HNO3 (3:1 vol/vol) solution at 35°C, stirred for twelve hours, and sonicated for 1 h. The solution was filtered and washed with double distilled water and acetone until the pH reached 6-7. The resulting oxidized graphene (o-graphene) was then dried under vacuum at 80°C for 12 h.

2.3. Silanization of graphene with 3-aminopropyltrithoxysilane

One gram of the o-graphene was dispersed in a 4% silane solution consisting of 3-APTES in double distilled water, which was then added to 300 mL of an ethanol:water (95:5 vol/vol) solution. The mixture was continuously stirred at 70°C for 2 h. The resulting functionalized graphene (f-graphene) was obtained by filtration using distilled water and acetone followed by drying at 90°C for 12 h. A schematic representation of the silanization process is given in Fig. 1.

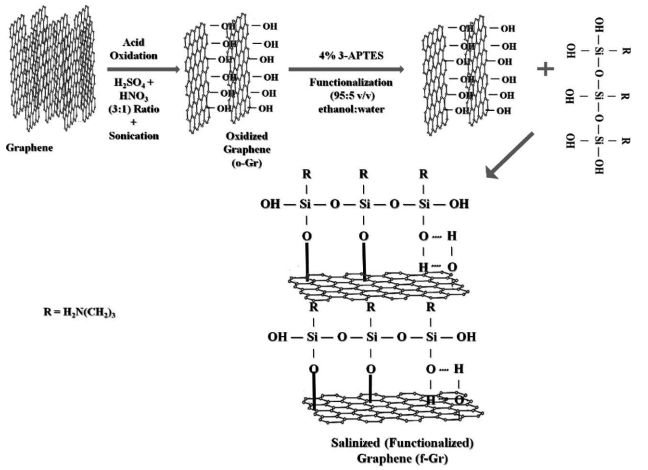

Fig. 1. Schematic representation of silanization process of graphene via hydrolysis of 3-aminopropyltriethoxysilane

2.4. Characterization

XRD patterns of graphene powder were recorded with a Rigaku Rotaflex (RU-200B) X-ray diffractometer using Cu Kα radiation with a Ni filter. The tube current and voltage were 300 mA and 40 kV, respectively and data from the 2θ angular regions between 20° and 80° were collected. Fourier transform Infrared (FT-IR) spectra were recorded using KBr pellets of raw graphene, o-graphene, and f-graphene on a Jasco FT-IR spectrometer. Raman analysis of the raw graphene, o-graphene, and f-graphene were carried out with a Jasco Raman spectrometer equipped with a 532 nm laser and a charge-coupled device (CCD) detector from 100 to 3200 cm-1. Thermal stability of the graphene powder was investigated using a thermogravimetric analysis (TGA) instrument (SDT Q600) under a nitrogen atmosphere at a heating rate of 5°C/min from 30°C to 1000°C. The surface morphology of raw graphene, o-graphene, and f-graphene were studied using an atomic force microscope (AFM) (Veeco D300, USA).

3. Results and discussion

3.1. XRD analysis

XRD was used to gather structural information for raw graphene, o-graphene, and f-graphene, and to assess the presence of metallic impurities. Fig. 2 shows the XRD patterns for raw graphene, o-graphene, and f-graphene. The peak at 2θ = 26.6° corresponds to the (002) graphitic carbon in graphene (JCPDF card no. 250284) [16-20]. The narrow peak at 2θ angle of 26° in the XRD patterns for raw graphene indicates the highly crystalline nature of graphene layers. A very small intensity peak is also observed at 2θ angle of 54.7° indicating the existence of the (004) graphene plane corresponding to the JCPDF card # 250284 respectively. Whereas, the (002) peak in o-graphene shows the decrease in peak intensity along with shifts in peak at 2θ angle of 26.7 respectively. One can notice the increase and shift in the intensity of peak at 2θ angle of 54.8° corresponding to the (004) graphene plane. The peak shifts and changes in intensity help us understand the presence of deformities and modification of sample crystallinity caused by chemical or mechanical treatments [21]. The f-graphene diffractograms shows that after salinization of o-graphene, reduced intensity of the (002) peak, and also the emergence of amorphous peaks at 2θ angles of 42°, 44°, and 77°. These correspond to the (100), (101), and (110) planes of graphite coupled with silane groups respectively.

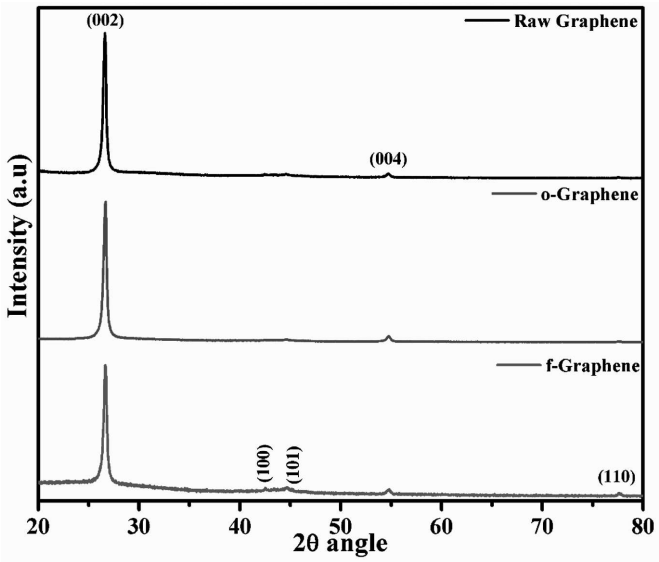

Fig. 2. XRD scans of raw graphene, oxidized graphene and functionalized graphene

3.2. FT-IR analysis

The FT-IR spectrum of raw graphene, shown in Fig. 3(a), shows that the graphite surface is devoid of any surface modifications and attachments. The peak at 3604 cm-1 is attributed to O-H bonds and indicates the presence of surface-absorbed moisture. The peaks at 3098, 1574, and 1163 cm-1 are attributed to the symmetrical stretching of C-H, C=C, and C-O bonds respectively [19, 22]. Fig. 3(b) shows the FT-IR spectrum of the acid-oxidized graphene sample. The spectrum shows the presence of a peak at 3439 cm-1 and the emergence of a strong

peak at 1382 cm-1 respectively [23]. This is attributed to the O-H symmetrical stretching, which indicates the presence of absorbed water. The emergence of this peak indicates the possible activation of the graphene surface for chemical bonding. The emergence of yet another small peak at 1703 cm-1 confirms the oxidation of the graphene surface. This peak, absent in raw graphene is attributed to the symmetrical stretching of C-O [19, 22]. Fig. 3(c) represents the FT-IR spectrum of the 3-APTES-functionalized graphene sample. The peaks at 1059 and 787 cm-1 can be attributed to the stretching of Si-O and Si-OH bonds respectively and indicates the presence of functionalized moieties (silane group in this case) [24]. The peaks at 3615, 1772, 1574, and 1163 cm-1 can be attributed to the presence O-H, C=O, C=C, and C-O stretching on the surface of the functionalized graphene respectively [19, 22]. The presence of all the above-mentioned vibrations, including those of the silane group, confirms the functionalization of graphene using this facile route.

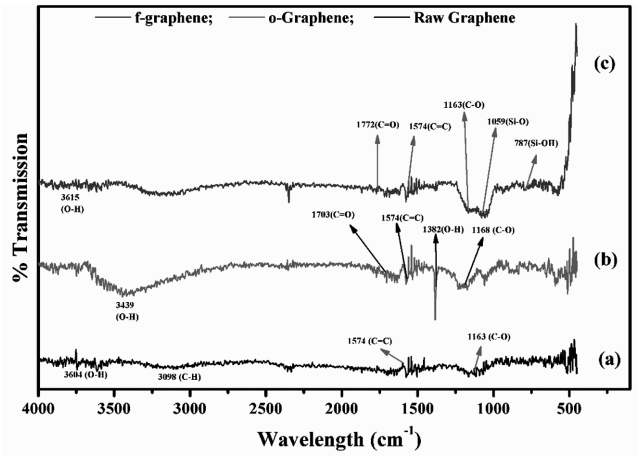

Fig. 3. FT-IR spectrum of (a) Raw graphene, (b) acid oxidized, (c) silanized graphene

3.3. Raman Analysis

The Raman spectra of (a) raw graphene, (b) o-graphene, (c) and f-graphene are shown in Fig. 4 from the spectra, one can notice the downward shift and broadening of the G-band peak post the chemical treatment of raw graphene. This downward blue shift and peak broadening of the G-band from 1581 to 1579 cm-1 in f-graphene shows that the graphene surface has been functionalized with the silane group [25, 26]. Thus, the covalent bonds formed with the oxidized surface lie within the (002) plane of graphene. This result is in agreement with the XRD results. One can also observe the increase in the intensity of the D-band peak, which indicates the presence of structural defects owing to functionalization. Another important observation is that the 2D peak that is generally observed at 2725 cm-1 also shows a downward shift and a decrease in intensity [25, 26]. This primarily suggests that the raw graphene is a few layers thick. The FWHM of the 2D peak is a function of the graphene thickness, i.e. the broader and shorter the peak, the greater the number of layers. As the oxidation and functionalization of graphene proceeds, the peak intensity, peak shifting, and broadening also decreases[25, 26] This further indicates the chemical exfoliation of the layers and introduction of dangling bonds due to oxidation. After the functionalization step, one can observe a larger decrease in the peak intensity, peak shifting, and broadening of the 2D peak. This is believed to be because of the formation of covalent bonds between the oxidized layers of graphene and the 3-APTES (silane group), resulting in the stacking [27, 28] and formation of multilayers of 3-APTES-Graphene nanocomposites (f-graphene). The proposed scheme of the chemical reaction is depicted in Fig. 1.

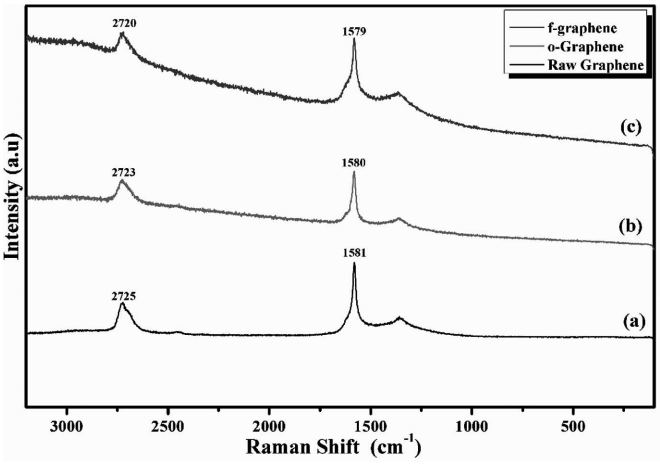

Fig. 4. Raman spectrum of (a) Raw graphene, (b) acid oxidized, (c) silanized graphene

3.4. Thermogravimetric analysis

Thermogravimetric analysis curves of raw graphene, oxidized graphene, and functionalized graphene are shown in Fig. 5. The thermal degradation of graphene powder is a multistep process that depends on the number of graphene layers present. The adsorbed water molecules on the graphene surface are reported to evaporate in the temperature range of 50-150°C. Decarboxylation starts in the temperature range of 150-350°C [19, 29]. The elimination of the hydroxyl groups attached to the graphene powder occurs in the temperature range of 350-500°C. Thermal oxidation of the remaining disordered carbon sites takes place around 550°C [30].

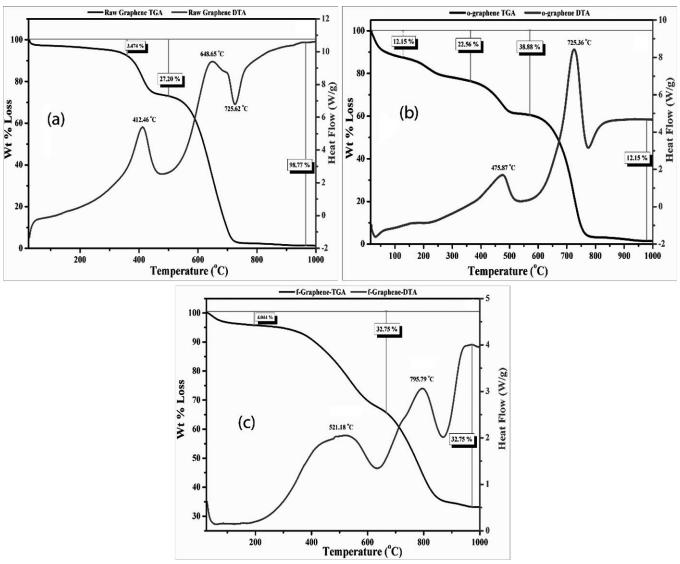

Fig. 5. TGA curves of raw graphene, oxidized graphene and silanized graphene, with a heating rate 5°C min-1 under nitrogen condition

TGA of the graphene powders clearly indicates higher thermal degradation for raw graphene due to the presence of adsorbed water, carboxyl groups, and, most importantly, the higher proportion of defective carbon. The DTA peaks also show that the thermal degradation is a highly exothermic reaction resulting in two major peaks between 400 and 460°C for raw graphene and o-graphene respectively. After functionalization, one can observe a delayed temperature response that shifts towards 512°C. This suggests that the silane group is masking the graphene layers and is thermally stable up to higher temperatures. A similar instance is observed in the second exothermic reaction around 795°C. The weight loss observed also shows the protective and the covalent chemical nature of the silane group towards graphene.

3.5. Atomic force microscopy

Atomic force microscopy images of o-graphene and f-graphene are shown in Fig. 6. Image analysis (Figs. 6a and 6b) reveals that the length and the diameter of an o-graphene flake is around 175 nm and 8 nm, respectively. The evaluated thickness is found to be around 0.093 nm, which suggests that the possible number of layers is two or three. This reduction in the number of layers can be attributed to the exfoliation caused by chemical oxidation and sonication.

Figs. 6c and 6d show the AFM image of f-graphene samples. Analysis reveals that the flake length is approximately 585 nm with a maximum diameter of around 11 nm. The average thickness of the functionalized flake is approximately 0.3 nm. This suggests that the covalent bonding between the silane group and the graphene surface caused stacking of the functionalized flakes in several layers. Thus, these results suggest that the functionalization of graphene with 3-APTES was successful.

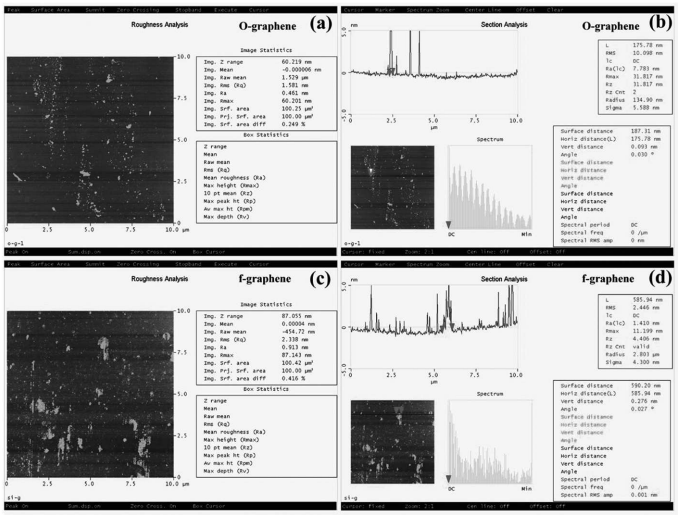

Fig. 6. AFM images of oxidized graphene and silanized graphene, demonstrating its roughness and sectional analysis

4. Conclusions

A facile route was employed to effectively functionalize the graphene surface using organosilane (3-APTES). The use of this simple procedure where graphene is first oxidized using mineral acid and then functionalized with organosilane resulted in impurity-free functionalized graphene. These f-graphene samples can be used to improve and enhance the chemical affinity, bonding and adhesion to the matrix. We envision that this functionalized graphene can have diverse applications in several fields of mechanical, electrical, and medical engineering.

Acknowledgements

This work was financially supported by the R & D project of "Development of Desalination Plant using Ocean Thermal Energy" supported by the Korea Research Institute of Ships & Ocean Engineering.

REFERENCES

[1] A.K. Geim, K.S. Novoselov, Nat. Mater. **6**, 183 (2007).
[2] K.S. Novoselov, A.K. Geim, S.V. Morozov, D. Jiang, Y. Zhang, S.V. Dubonos, I.V. Grigorieva, A.A. Firsov, Science. **306**, 666 (2004).
[3] Y.B. Zhang, Y.W. Tan, H.L. Stormer, P. Kim, Nature. **438**, 201 (2005).
[4] A.A. Balandin, S. Ghosh, W. Bao, I. Calizo, D. Teweldebrhan, F. Miao, C.N. Lau, Nano. Lett. **8**, 902 (2008).
[5] J. Moser, A. Barrieiro, A. Bachtold, Current-induced cleaning of graphene, Appl. Phys. Lett. **91**, 163513 (2007).
[6] J.R. Potts, D.R. Dreyer, C.W. Bielawski, R.S. Ruoff, Polymer. **52**, 5 (2011).
[7] G. Eda, M. Chhowalla, Nano. Lett. **9**, 814 (2009).
[8] B. Das, K.E. Prasad, U. Ramamurty, C. Rao, Nanotechnology. **20**, 125705 (2009).
[9] K.E. Prasad, B. Das, U. Maitra, U. Ramamurty, C. Rao, PNAS. **106**, 13186 (2009).
[10] J. Guo, L. Ren, R. Wang, C. Zhang, Y. Yang, T. Liu, Compos. Part B-Eng. **42**, 2130 (2011).
[11] G.W. Jeon, J.E. An, Y.G. Jeong, Compos. Part B-Eng. **43**, 3412 (2012).
[12] M.A. Rafiee, J. Rafiee, Z. Wang, H. Song, Z.Z. Yu, N. Koratkar, ACS Nano **3**, 3884 (2009).
[13] H. Chen, M.B. Müller, K.J. Gilmore, G.G. Wallace, D. Li, Adv. Mater. **20**, 3557 (2008).
[14] J. Kathi, K.Y. Rhee, J. Mater. Sci. **43**, 33 (2008).
[15] P.C. Ma, J.K. Kim, B.Z. Tang, Carbon. **44**, 3232 (2006).
[16] P. Mahanandia, P. Vishwakarma, K. Nanda, V. Prasad, S. Subramanyam, S. Dev, P.V. Satyam, Mater. Res. Bull. **41**, 2311 (2006).
[17] V. Labunov, B. Shulitski, A. Prudnikava, K. Yanushkevich, J. Phys. Conf. Ser. **100**, 052095 (2008).
[18] W. Li, C. Liang, W. Zhou, J. Qiu, Z. Zhou, G. Sun, Q. Xin, J. Phys. Chem. B. **107**, 6292 (2003).
[19] J.N. Ding, Y.B. Liu, N.Y. Yuan, G.Q. Ding, Y. Fan, C.T. Yu, Diamond Relat. Mater. **21**, 11 (2012).
[20] S. Gurunathan, J.W. Han, A.A. Dayem, V. Eppakayala, M.R. Park, D.N. Kwon, J.H. Kim, J. Ind. Eng. Chem. **19**, 1280 (2013).
[21] S.H. Song, H.K. Jeong, Y.G. Kang, J. Ind. Eng. Chem. **16**, 1059 (2010).
[22] X. Li, Y. Zhao, W. Wu, J. Chen, G. Chu, H. Zou, J. Ind. Eng. Chem. (2013), DOI: 10.1016/j.jiec.2013.09.029 (in press).
[23] S. Bittolo Bon, M. Piccinini, A. Mariani, J.M. Kenny, L. Valentini, Diamond Relat. Mater. **20**, 871 (2011).

[24] S. Hou, S. Su, M.L. Kasner, P. Shah, K. Patel, C.J. Madarang, Chem. Phys. Lett. **501**, 68 (2010).
[25] M. Castriota, E. Cazzanelli, D. Pacilè, L. Papagno, Ç. O. Girit, J.C. Meyer, A. Zettl, M. Giarola, G. Mariotto, Diamond Relat. Mater. **19**, 608 (2010).
[26] S. Takabayashi, S. Ogawa, Y. Takakuwa, H.C. Kang, R. Takahashi, H. Fukidome, M. Suemitsu, T. Suemitsu, T. Otsuji, Diamond Relat. Mater. **22**, 118 (2012).
[27] Y. Min, K. Zhang, L. Chen, Y. Chen, Y. Zhang, Diamond Relat. Mater. **26**, 32 (2012).
[28] Y. Hsieh, M. Hofmann, J. Kong, Carbon. **67**, 417 (2014).
[29] J. Shen, Y. Hu, C. Li, C. Qin, M. Shi, M. Ye, Langmuir. **25**, 6122 (2009).
[30] G. Wang, J. Yang, J. park, X. Gou, B. Wang, H. Liu, J. Yao, J. Phys. Chem. B. **112**, 8192 (2008).

Received: 20 November 2014.